INFECTION AND IMMUNITY, June 2008, p. 2620–2632 Vol. 76, No. 6
0019-9567/08/$08.00+0 doi:10.1128/IAI.01308-07

Identification and Characterization of a Repeat-in-Toxin Gene Cluster in *Vibrio anguillarum*▽

Ling Li, Jessica L. Rock,† and David R. Nelson*

Department of Cell and Molecular Biology, University of Rhode Island, Kingston, Rhode Island 02881

Received 26 September 2007/Returned for modification 16 January 2008/Accepted 24 March 2008

Vibrio anguillarum **is the causative agent of vibriosis in fish. Hemolysins of *V. anguillarum* have been considered virulence factors during infection. One hemolysin gene, *vah1*, has been previously identified but does not account for all hemolytic activity. The mini-Tn*10*Km mutagenesis performed with a *vah1* mutant resulted in a hemolysin-negative mutant. The region surrounding the mutation was cloned and sequenced, revealing a putative *rtx* operon with six genes (*rtxACHBDE*), where *rtxA* encodes an exotoxin, *rtxC* encodes an RtxA activator, *rtxH* encodes a conserved hypothetical protein, and *rtxBDE* encode the ABC transporters. Single mutations in *rtx* genes did not result in a hemolysin-negative phenotype. However, strains containing a mutation in *vah1* and a mutation in an *rtx* gene resulted in a hemolysin-negative mutant, demonstrating that the *rtx* operon is a second hemolysin gene cluster in *V. anguillarum* M93Sm. Reverse transcription-PCR analysis revealed that the *rtxC* and *rtxA* genes are cotranscribed, as are the *rtxBDE* genes. Additionally, Vah1 and RtxA each have cytotoxic activity against Atlantic salmon kidney (ASK) cells. Single mutations in *vah1* or *rtxA* attenuate the cytotoxicity of *V. anguillarum* M93Sm. A *vah1 rtxA* double mutant is no longer cytotoxic. Moreover, Vah1 and RtxA each have a distinct cytotoxic effect on ASK cells, Vah1 causes cell vacuolation, and RtxA causes cell rounding. Finally, wild-type and mutant strains were tested for virulence in juvenile Atlantic salmon. Only strains containing an *rtxA* mutation had reduced virulence, suggesting that RtxA is a major virulence factor for *V. anguillarum*.**

Vibrio anguillarum is a highly motile gram-negative, curved rod bacteria. This marine member of the class *Gammaproteobacteria* is one of the causative agents of vibriosis, a fatal hemorrhagic septicemic disease in fish, crustaceans, and bivalves (1). Fish infected with *V. anguillarum* display skin discoloration and erythema around the mouth, fins, and vent. Necrotic lesions are observed in the abdominal muscle (14). Mortality rates for infected fish populations may range from 30% to as high as 100% (1). Vibriosis has resulted in severe economic losses to aquaculture worldwide (1, 45) and affects many farm-raised fish including Pacific salmon, Atlantic salmon, sea bass, cod, and eel (1, 14, 18, 45).

Several genes have been reported to be correlated with the virulence of *V. anguillarum*, such as the *vah1* hemolysin gene cluster (40), the siderophore-mediated iron transport system (16), the *empA* metalloprotease gene (15, 36), and the *flaA* gene (37). The hemolytic activity of *V. anguillarum* has been considered the virulence factor responsible for hemorrhagic septicemia during infection (27). Hirono et al. (27) identified the first hemolysin gene, *vah1*, in *V. anguillarum* and suggested that the *vah1* gene is broadly distributed among *V. anguillarum* strains. Rock and Nelson (40) described a *vah1* gene cluster in *V. anguillarum* strain M93Sm, in which the *vah1* gene was linked to two putative lipase-related genes (*llpA* and *llpB*) and a hemolysin-like gene (*plp*) that appeared to function as a repressor of hemolytic activity. Furthermore, mutations in the *vah1* cluster of genes did not result in the loss of hemolytic activity, suggesting that *V. anguillarum* contained more than one hemolysin (40). Additionally, Rodkhum et al. (41) found that *V. anguillarum* strain H775-3 contained four hemolysin genes (*vah2*, *vah3*, *vah4*, and *vah5*) in addition to *vah1*. The encoded proteins showed strong similarities to hemolysins of *V. vulnificus* (*vah2*) and *V. cholerae* (*vah3*, *vah4*, and *vah5*).

The repeat-in-toxin (RTX) family is a group of related protein toxins found in gram-negative bacteria. These toxins have a broad range of distribution and activities, which includes *Escherichia coli* HlyA hemolytic toxin (2, 35), *V. cholerae* RtxA cytotoxin (32), *V. vulnificus* RtxA cytotoxin (31), *Bordetella pertussis* CyaA adenylate cyclase (26), *Pseudomonas aeruginosa* alkaline protease (3), and *Actinobacillus pleuropneumoniae* Apx toxin (28, 29). These toxin genes usually form an operon and share some common features, such as posttranslational maturation by acylation, a C-terminal calcium-binding domain with tandem glycine/aspartic acid-rich repeats, and secretion of the toxin facilitated by type I secretion systems (TISS) (6). Studies demonstrate that the *rtx* operons are commonly found in *Vibrio* species. Lin et al. (32) first identified an *rtx* operon in *V. cholerae* and showed that the Rtx toxin caused HEp-2 cells to round up. Further research demonstrated that the Rtx toxin in *V. cholerae* was responsible for the covalent cross-linking of cellular actin (22), and an actin cross-linking domain (ACD) was recently discovered in the RtxA protein of *V. cholerae* (11). The *rtx* operon was also found in *V. vulnificus* where it functioned as a cytotoxin (31). Lee et al. (31) showed that *V. vulnificus* virulence in mice was dependent on *rtxA*. Recently, Satchell (42) renamed the RtxA toxin of *V. cholerae* the multifunctional autoprocessing Rtx toxin (MARTX). This new family of RtxA toxins exhibits highly conserved structural domains and variable catalytic activity domains assembled as mosaics. MARTX toxins are found in at least eight gram-negative

* Corresponding author. Mailing address: Department of Cell and Molecular Biology, University of Rhode Island, Kingston, RI 02881. Phone: (401) 874-5902. Fax: (401) 874-2202. E-mail: dnelson@uri.edu.
† Present address: Cubist Pharmaceuticals, 65 Hayden Ave., Lexington, MA 02421.
▽ Published ahead of print on 31 March 2008.

TABLE 1. Bacterial strains and plasmids used in this study

Strain or plasmid	Genotype and feature(s)	Reference
V. anguillarum strains		
M93Sm	Spontaneous Sm^r mutant of M93 (serotype J-O-1)	13
S123	Sm^r Cm^r; M93Sm *rtxA* mutant	This study
S189	Sm^r Cm^r; M93Sm *rtxC* mutant	This study
S103	Sm^r Cm^r; M93Sm *rtxB* mutant	This study
S191	Sm^r Cm^r; M93Sm *rtxD* mutant	This study
S206	Sm^r Cm^r; M93Sm *rtxE* mutant	This study
S171	Sm^r Kan^r; M93Sm *vah1* mutant	This study
S183	Sm^r Cm^r Kan^r; M93Sm *rtxA vah1* double mutant	This study
S193	Sm^r Cm^r Kan^r; M93Sm *rtxC vah1* double mutant	This study
JR7	Sm^r Cm^r Kan^r; M93Sm *rtxB vah1* double mutant	This study
S195	Sm^r Cm^r Kan^r; M93Sm *rtxD vah1* double mutant	This study
S208	Sm^r Cm^r Kan^r; M93Sm *rtxE vah1* double mutant	This study
E. coli strains		
Sm10	*thi thr leu tonA lacY supE recA* RP4-2-Tc::Mu::Km (λ *pir*)	36
S156	Sm10 containing plasmid pLL1106	This study
Plasmids		
pNQ705-1	Cm^r; suicide vector with R6K origin	37
pDM4	Cm^r Kan^r $SacBC^r$; suicide vector	37
pJR7	pBlueScript with partial *rtx* operon (for sequence)	This study
pBLUEscript	Cloning vector	Stratagene
pLL1106	pDM4 containing the 5′ and 3′ parts of *vah1* (for allelic exchange mutagenesis)	This study

bacterial species, including members of the genera *Vibrio*, *Aeromonas*, and *Yersinia* (42).

In this study, we sought to identify and characterize genes in addition to *vah1* that contribute to the hemolytic activity of *V. anguillarum* M93Sm. Minitransposon mutagenesis was used to create and screen for hemolysin-negative mutants in a *vah1* mutant background. One mutant that exhibited negative hemolytic activity was obtained, and the region surrounding this mutation was cloned and sequenced. A putative *rtx* operon was identified and characterized. Additionally, the contributions of the Vah1 and the Rtx hemolysins to cytotoxicity in Atlantic salmon kidney (ASK) cells and to virulence in juvenile Atlantic salmon were determined.

MATERIALS AND METHODS

Bacterial strains, plasmids, and growth conditions. All bacterial strains and plasmids used in this report are listed in Table 1. *V. anguillarum* strains were routinely grown in Luria-Bertani broth plus 2% NaCl (LB20) (23), supplemented with the appropriate antibiotic, in a shaking water bath at 27°C. Overnight cultures of *V. anguillarum* were grown in LB20 and centrifuged (8,000 × *g*, 10 min), and pelleted cells were washed twice with nine-salt solution (NSS) (23). Washed cells were resuspended to appropriate cell densities in experimental medium. Specific conditions are described in the text for each experiment. Antibiotics were used at the following concentrations: streptomycin, 200 μg/ml; chloramphenicol, 20 μg/ml for *E. coli* and 5 μg/ml for *V. anguillarum*; kanamycin, 80 μg/ml; ampicillin, 100 μg/ml; tetracycline, 2 μg/ml.

Bacterial mating. Plasmids were introduced into *V. anguillarum* M93Sm from *E. coli* Sm10 (λ *pir*) by conjugation procedures described previously (37). Briefly, aliquots (100 μl) from overnight cultures of *V. anguillarum* and *E. coli* Sm10 were mixed at ratios of 1:1 in 2.5 ml of NSS plus 2.5 ml 10 mM $MgSO_4$. The cell mixture was vacuum filtered onto a 0.45-μm-pore-size filter, which was placed on an LB15 agar plate (Luria-Bertani agar plus 1.5% NaCl) and allowed to incubate overnight at 27°C. Following incubation, the cells were removed from the filter by vigorous vortexing in 5 ml NSS. The cell suspension was spread on appropriate selection plates and allowed to incubate at 27°C until *V. anguillarum* colonies were observed.

Mini-Tn*10*Km mutagenesis. Mini-Tn*10*Km mutagenesis was carried out by using a method developed by Herrero et al. (25), with a modification (40). Briefly, *V. anguillarum* M93Sm was mated with *E. coli* CC118 (λ *pir*)(pLOFKm) containing the mini-Tn*10*Km according the procedures described above. The transconjugants were selected onto LB20 plates supplemented with 200 μg/ml streptomycin (Sm^{200}) and 80 μg/ml kanamycin (Kan^{80}) for *V. anguillarum* mutants containing a mini-Tn*10*Km insertion. *V. anguillarum* colonies able to grow on LB20-Sm^{200}-Kan^{80} were transferred onto trypticase soy agar (TSA)-sheep blood agar plates, and hemolytic activity was determined by measuring β-hemolysis after 24 h at 27°C.

Cloning of the mini-Tn*10*Km insertion mutation. The region surrounding the gene, interrupted by the mini-Tn*10*Km mutagenesis, was cloned into pBluescript $SKII^+$ (Stratagene). Briefly, genomic DNA from *V. anguillarum* strain JR7 was extracted and digested with SacI, and digestion fragments were ligated into the SacI-digested site of pBluescript $SKII^+$. Then, the ligated DNA was transformed into *E. coli* XL1 MRF′ by electroporation, using a Bio-Rad gene pulser (at 1.5 kV, 25 μF, 200 Ω). Transformants were selected on LB agar plates supplemented with 100 μg/ml ampicillin. Plasmid DNA was purified from the clone using a Qiagen Mini-Prep kit (Qiagen). The plasmids were checked for the presence of inserted *V. anguillarum* DNA containing mini-Tn*10*Km by restriction digestion, followed by agarose gel electrophoresis. Clones of interest were saved for future study and sequencing.

Construction of the *vah1*::*Km* allelic exchange mutation. The plasmid pDM4 (generously provided by Debra Milton) was used to construct the *vah1*::*Km* allelic exchange mutant as described previously by Milton et al. (37). The kanamycin resistance gene was amplified from the TOPO2.1 vector (Invitrogen) with the primer pair Pm152 and Pm153 (Table 2) and inserted into the XbaI and SphI sites of pDM4. The 5′ and 3′ regions of *vah1* were amplified by PCR and inserted into either side of the kanamycin gene. The 5′ flanking region of *vah1* was amplified from M93Sm genomic DNA with the primer pair Pm156 and Pm157 (Table 2), which amplified a 489-bp product and introduced XhoI and XbaI sites at the ends of the PCR product. The 3′ flanking region was amplified from M93Sm genomic DNA with the primer pair Pm154 and Pm155 (Table 2), which amplified a 469-bp product and introduced SphI and SacI sites at the ends of the PCR product. Both of these PCR products were cloned, sequenced, and subcloned on either side of the kanamycin resistance gene to produce the pDM4 derivative plasmid pLL1106, which was transformed into *E. coli* Sm10 (λ pir) to produce the transformant strain S156. S156 was mated with *V. anguillarum* M93Sm, and the double-crossover transconjugants were selected with LB20-Kan^{80}-Sm^{200}-5% sucrose plates. The resulting *V. anguillarum* mutants were checked for the desired allelic exchange using PCR amplification and restriction enzyme digestion. The mutant was designated S171 and used in further studies.

Insertional mutagenesis by homologous recombination of the *rtx* genes. Insertional mutagenesis by homologous recombination was used to create gene interruptions within the structural genes of the *rtx* operon by integrating a

TABLE 2. Primers used in this study

Primer[a]	Sequence (5′–3′)[b]	Target[c]
Pm105	ATCGAGAGCTCGCAAAATTCATGCTTATG	*rtxA* insertion mutation
Pm108	ATCGATCTAGAGTTGTAAGCCGCAGCAC	*rtxA* insertion mutation
Pm180	ATCGAGAGCTCGATCGTGCAATGATGCAG	*rtxC* insertion mutation F
Pm181	ATCGATCTAGAGCGGCTTCGATTTCTCGT	*rtxC* insertion mutation R
SD *rtxB* F2	GCTAGGAGCTCGTTGCGATAATTCAGGT	*rtxB* insertion mutation
SD *rtxB* R2	GCTAGTCTAGATACCGCTGATCGGAATCGT	*rtxB* insertion mutation
Pm182	ATCGAGAGCTCGCGTATTTGATGACGCAAAC	*rtxD* insertion mutation F
Pm183	ATCGATCTAGAGCTCACCTTACTTTGGACCT	*rtxD* insertion mutation R
Pm190	ATCGAGAGCTCGGATTTTGACCAATGCAGGT	*rtxE* insertion mutation
Pm191	ATCGATCTAGACATTAGCGGCCCTCTCGTT	*rtxE* insertion mutation
Pm152	ATCGATCTAGAGAACACGTAGAAAGCCAGT	*kan* cassette amplification
Pm153	ACTGAGCATGCTCAGAAGAACTCGTCAAGAA	*kan* cassette amplification
Pm156	ATCGACTCGAGATGTCAATAAACAGAAGAAA	*vah1* allelic exchange 5′ flanking
Pm157	ATCGATCTAGAGTTCGTTTCCGAACCACTAT	*vah1* allelic exchange 5′ flanking
Pm154	ATCGAGCATGCGGTTCATTGGCCTTACAA	*vah1* allelic exchange 3′ flanking
Pm155	ATCAGGAGCTCGATAAAATTAACATCGAATTAAC	*vah1* allelic exchange 3′ flanking
Pm111	GGAAATTATTCCGCCGACGATGGA	*rtxA* RT-PCR F
Pm112	GCCGATACCGTATCGTTACCTGAA	*rtxA* RT-PCR R
Pm180 (RT)	GATCGTGCAATGATGCAG	*rtxC* RT-PCR F
Pm181 (RT)	GCGGCTTCGATTTCTCGT	*rtxC* RT-PCR R
Pm184	GTTGTAGATGCGTGCCTTGCTCTG	*rtxB* RT-PCR
Pm185	CCAATATGGAGCAAATTGCCGCCG	*rtxB* RT-PCR
Pm182 (RT)	GCGTATTTGATGACGCAAAC	*rtxD* RT-PCR F1
Pm183 (RT)	GCTCACCTTACTTTGGACCT	*rtxD* RT-PCR R2
Pm187	GAGCGGGAAAAACCAACCCAAGT	*rtxD* RT-PCR F3
Pm189	GTGTTCACACCCTTGGGGCAGTC	*rtxD* RT-PCR R4
Pm190 (RT)	GGATTTTGACCAATGCAGGT	*rtxE* RT-PCR
Pm191 (RT)	CATTAGCGGCCCTCTCGTT	*rtxE* RT-PCR

[a] RT, reverse-transcription primer.
[b] Restriction sites for SacI (GAGCTC), XbaI (TCTAGA), SphI (GCATGC), and XhoI (CTCGAG) are underlined.
[c] F, forward; R, reverse.

plasmid into each *rtx* gene. Primers (Table 2) were designed based on the *rtx* gene sequence of M93Sm (GenBank accession no. EU155486). For the construction of the *rtxA* mutant, a 281-bp DNA fragment was PCR amplified by using primers Pm105 and Pm108 (Table 2) and cloned into the suicide vector pNQ705 by using SacI and XbaI restriction endonucleases to yield the pNQ705 derivative plasmid pLL1037, which was confirmed by both PCR amplification and restriction analysis. The mobilizable suicide vector was transferred from *E. coli* Sm10 containing plasmid pLL1037 into *V. anguillarum* M93Sm by conjugation. Transconjugants were selected by utilizing the chloramphenicol resistance gene located on the suicide plasmid. The incorporation of the suicide vector into the *rtxA* gene was confirmed by PCR analysis, as described previously by Milton et al. (37). The resulting *V. anguillarum rtxA* mutant was designated S123 (Table 1). For creating the *rtxC*, *rtxB*, *rtxD*, and *rtxE* mutants, specific DNA fragments were amplified separately and used in the same protocol as that used for the *rtxA* gene interruption.

RT-PCR. The *V. anguillarum* wild-type strain M93Sm was grown to exponential phase ($\sim 2 \times 10^8$ CFU/ml), and 1 ml of cells was harvested by centrifugation at 8,000 × *g* for 10 min. Total RNA was isolated using an RNeasy kit (Qiagen) according to the manufacturer's instructions. Isolated RNA was treated with DNase and used as the template (a 1-μg-per-50-μl reaction mixture) for reverse transcription (RT)-PCR. RT-PCR was performed using Brilliant SYBR Green single-step quantitative RT-PCR (qRT-PCR) Master Mix (Stratagene). Briefly, gene-specific primers (Table 2) were used to reverse transcribe the specific cDNA from RNA templates, and the resulting cDNA was used as the template with which to amplify the specific DNA product, using the regular PCR method. Genomic DNA (1 μg) extracted from wild-type strain M93Sm was used as the positive control. The reaction mixture without the addition of reverse transcriptase was used as a negative control. The thermal profile was 50°C for 30 min and 95°C for 15 min and then 35 cycles of 95°C for 30 s, 55°C for 30 s, and 72°C for 30 s. PCR product was visualized in a 1% agarose gel with a 100-bp DNA molecular weight ladder (Promega).

DNA sequencing. All DNA sequencing was done at the URI Genomics and Sequencing Center (University of Rhode Island, Kingston, RI), using an ABI3170xl Genetic Analyzer unit (Applied Biosystems).

Complementation of the *rtx* mutants. The *rtx* gene fragments were cloned to test the ability to complement the various *rtx* gene mutants, as described previously by Rock and Nelson (40). The mutants were complemented by cloning the appropriate genes into the shuttle vector pSUP202 (GenBank accession no. AY428809). Briefly, total genomic DNA from *V. anguillarum* M93Sm was isolated. A restriction site (PstI or EcoRI) was chosen according to the *rtx* operon sequence data (GenBank accession no. EU155486) and added to the PCR primer set used to amplify the gene of interest plus the putative native promoter region (P_{native}), which is the 500-bp upstream region of the *rtxD* and *rtxE* genes and the whole intergenic region of the *rtxC* and *rtxB* genes (as shown in Fig. 4A). For making constitutive expressed *rtx* genes, a constitutive promoter for *flaB* (P_{flaB}) (17), which was confirmed to constitutively express in both *E. coli* and *V. anguillarum* (L. Li and D. R. Nelson, unpublished data), was used to create P_{flaB}-driven *rtx* genes (P_{flaB} mutant) (Fig. 4A). P_{flaB} was PCR amplified using plasmid pCE320(*gfp*)-P_{flaB} (kindly supplied by Christian Eggers) (17) as the template. The restriction site SpeI was added to the primer set, which was used to insert the *flaB* promoter in front of the *rtx* gene (an SpeI site was also added to the PCR primer sets). All PCR fragments were subcloned into the PCR2.1 vector and digested with the appropriate restriction enzyme. The gel-purified gene fragment was ligated into pSUP202 and transformed into *E. coli* Sm10. *E. coli* Sm10 containing various pSUP202 plasmid derivatives (Fig. 4A) was conjugated into various *rtx* gene mutants by using the procedures described above. The conjugants were confirmed by using PCR amplification and restriction digestion.

Cytotoxicity assay. ASK cells (ATCC CRL-2747) were seeded into a six-well microtiter plate (Costar) in Leibovitz's L-15 medium (ATCC) supplemented with 10% fetal bovine serum and grown at 20°C to a cell density of $\sim 2 \times 10^5$ cells ml^{-1}. *V. anguillarum* cultures grown overnight were harvested, washed twice in NSS, and resuspended in NSS (at a cell density of $\sim 2 \times 10^9$ cells ml^{-1}). The supernatant from the overnight culture was filtered though a 0.22-μm-pore-size filter (Millipore). Washed bacterial cells were added to ASK cells at various multiplicities of infection (MOI) and incubated at 20°C for up to 4 h. Filtered supernatant (1 ml) was added directly to ASK cells containing 1 ml fresh medium and incubated at 20°C for 4 h or overnight (20 h). Changes in cell morphology were assessed and photographed by viewing live cells with an inverted micro-

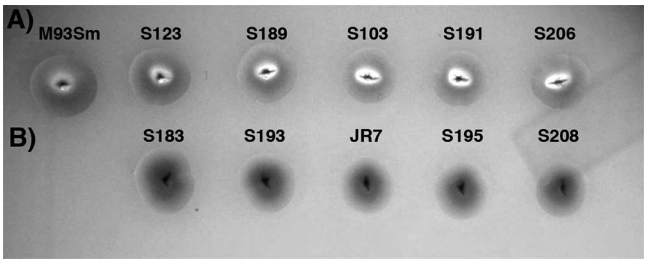

FIG. 1. Hemolytic activity of the wild-type *V. anguillarum* M93Sm and its hemolysin mutant strains with TSA-5% sheep blood agar. Mutations in single *rtx* genes did not eliminate the hemolytic activity of M93Sm (A); however, mutations in both the *vah1* and *rtx* genes resulted in the loss of hemolysin activity (B). All bacterial strains were transferred onto a sheep blood agar plate and incubated at 27°C for 48 h. S123, the *rtxA* mutant strain; S189, the *rtxC* mutant strain; S103, the *rtxB* mutant strain; S191, the *rtxD* mutant strain; S206, the *rtxE* mutant strain. S183, the *vah1 rtxA* double mutant strain; S193, the *vah1 rtxC* double mutant strain; JR7, the *vah1 rtxB* double mutant strain; S195, the *vah1 rtxD* double mutant strain; S208, the *vah1 rtxE* double mutant strain.

scope (Nikon TE2000 model). The concentration and viability of ASK cells were determined by the trypan blue dye exclusion method using a Vi-Cell cell viability analyzer (Beckman Coulter).

Fish infections. Hemolysin mutants were tested for virulence with juvenile Atlantic salmon (*Salmo salar* L.) by intraperitoneal (i.p.) injection, as described by Denkin and Nelson (14). Briefly, *V. anguillarum* cells grown in LB20 supplemented with appropriate antibiotics for 18 h at 27°C were harvested by centrifugation (8,000 × *g*, 10 min, 4°C), washed twice in NSS, and suspended in NSS. The cell density of NSS suspensions was determined by serial dilution and spot plating. Fifteen fish (10 to 15 cm long) were used to test the virulence of each bacterial strain. Seven fish were sham inoculated with NSS as a negative control. Fish inoculated with different bacterial strains were maintained in separate tanks to prevent possible cross-contamination. Five fish were inoculated per dose, and three different doses per strain were used. Fish were inoculated i.p. with 100 μl of cells (ranging from ~10^5 to 10^7 CFU ml^{-1}) in NSS or with NSS alone (control fish). The fish were anesthetized in water supplemented with tricaine methane sulfonate (100 mg ml^{-1}) prior to inoculation and allowed to recover before they were returned to their tanks. Death due to vibriosis was determined by the observation of gross clinical signs and confirmed by the recovery and isolation of *V. anguillarum* cells resistant to the appropriate antibiotics from infected organs of dead fish. Observations were made for 21 days. All fish used in this research project were obtained from the URI East Farm Aquaculture Center.

RESULTS

Mini-Tn*10*Km mutagenesis. Previously, Rock and Nelson (40) found that when the *vah1* hemolysin gene was mutated in *V. anguillarum* M93Sm, the resulting mutant exhibited little or no reduction in hemolytic activity. This result, coupled with the observation that a mutation in the adjacent and divergently transcribed *plp* gene increased both the *vah1* transcription and the hemolytic activity, implied that there was a second hemolysin. To identify additional hemolysin genes in *V. anguillarum* M93Sm, mini-Tn*10*Km mutagenesis (25) was carried out with *V. anguillarum* JR1 (Table 1), a *vah1* insertion mutant of M93Sm (40). Over 3,000 mini-Tn*10*Km-containing colonies were screened on sheep blood agar plates for altered hemolytic activity. One clone, designated JR7, exhibited negative hemolytic activity (Fig. 1). This indicated that an unknown gene, other than *vah1*, was disrupted by a mini-Tn*10*Km insertion and that the mutations in this gene and in *vah1* together resulted in the complete loss of hemolytic activity in *V. anguillarum* M93Sm.

Cloning and identification of the putative *V. anguillarum rtx* hemolysin genes. To identify the gene interrupted by the mini-Tn*10*Km insertion, genomic DNA from strain JR7 was isolated and digested with SacI (Fig. 2A). Digested DNA fragments were inserted into the SacI site of plasmid pBluescript IISK+ and then transformed into *E. coli* XL1MRF′. A fragment of ~13 kbp containing the kanamycin resistance gene was obtained, and the plasmid designated pJR7 was isolated for DNA

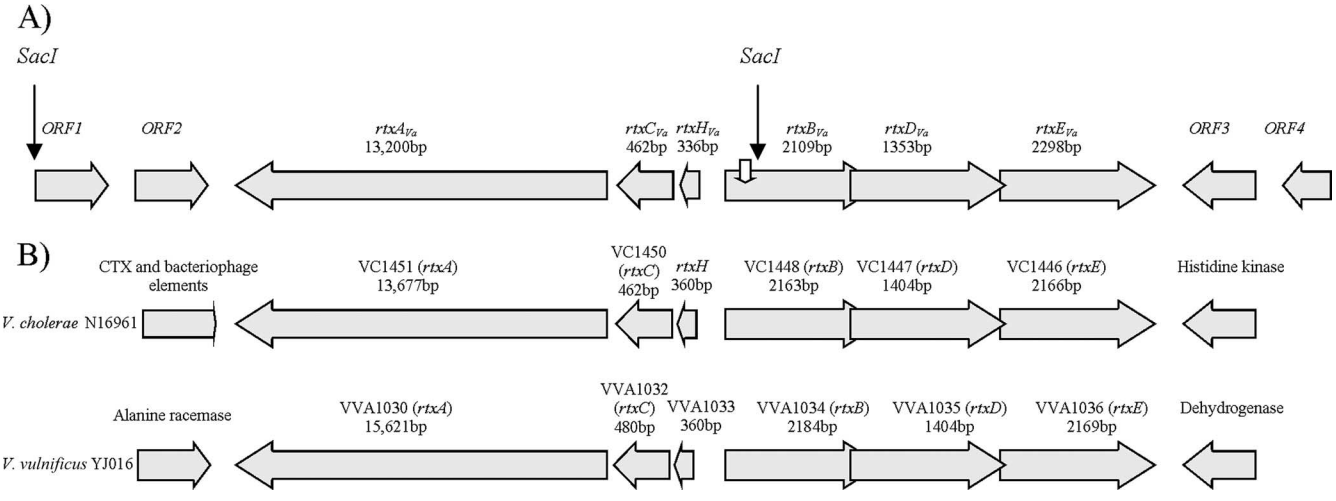

FIG. 2. Comparison of the *rtx* operon organization in *V. anguillarum* M93Sm (A) with that of *V. cholerae* and *V. vulnificus* (B). (A) The *rtx* operon and its flanking DNA in *V. anguillarum* M93Sm, as follows: $rtxA_{Va}$ encodes RtxA, a secreted toxin and virulence factor; $rtxC_{Va}$ is a putative acylase that acts as an $RtxA_{Va}$ activator; $rtxH_{Va}$ is a conserved hypothetical gene; $rtxBDE_{Va}$ are putative ABC transporters of $RtxA_{Va}$. The open arrow indicates the insertion of the kanamycin cassette by mini-Tn*10*Km mutagenesis in the $rtxB_{Va}$ gene in JR7 (the *vah1 rtxB* double mutant). The DNA fragment between the SacI sites was cloned into plasmid pJR7 and sequenced by primer walking. The rest of the DNA is cloned and sequenced using inverse PCR. Identifications based on BLASTx similarities, as follows: ORF1, nicotinate-nucleotide-dimethylbenzimidazole phosphoribosyltransferase; ORF2, cobalamin synthase; ORF3, chemotaxis gene; ORF4, Na-carboxylase symporter. (B) The *rtx* operon and its flanking genes in *V. cholerae* El Tor strain N16961 and *V. vulnificus* strain YJ016 (9). The diagram shows the arrangements are identical for the *rtx* operon and the distinct flanking genes of three *Vibrio* species.

TABLE 3. Homology analysis of the *rtx* operon of *V. anguillarum* and other species

ORF	Predicted no. of aa/ protein mass (kDa)	Accession no.	Homology to *rtx* genes of other species[a]							
			V. vulnificus YJ016				*V. vulnificus* CMCP6			
			% of identity/ % of similarity	Homologue locus	Putative function	Predicted size (aa)	% of identity/ % of similarity	Homologue locus	Putative function	Predicted size (aa)
$rtxA_{Va}$	4,399/467	EU155486	90/95	NP_937086	Cytotoxin	5,206	90/95	NP_762440	Adhesin	5,206
$rtxC_{Va}$	153/18	EU155486	75/89	NP_937088	Rtx acylase	159	75/89	NP_762441	Acyltransferase	153
$rtxH_{Va}$	111/12	EU155486	69/78	NP_937089	Hypothetical protein	119	69/78	NP_762442	Hypothetical protein	89
$rtxB_{Va}$	702/79	EU155486	67/80	NP_937090	ABC transporter	727	73/86	NP_762443	ABC transporter	535
$rtxD_{Va}$	450/51	EU155486	63/77	NP_937091	ABC transporter	467	62/77	NP_762444	ABC transporter	453
$rtxE_{Va}$	765/85	EU155486	71/84	NP_937092	ABC transporter	722	71/84	NP_762445	ABC transporter	722

[a] N/A, not applicable, no homology by BLASTx; aa, amino acid(s).

sequencing. Sequencing of the pJR7 plasmid revealed four complete open reading frames (ORFs) and one incomplete ORF (Fig. 2A). BLASTx analysis of the ORFs within this region (24) revealed a cluster of genes that displayed a high level of similarity to genes involved in the biogenesis of RTX toxins in several gram-negative organisms, including *V. cholerae* N16961 (GenBank accession number NP231094) (32) and *V. vulnificus* CMCP6 (GenBank accession number NP762440) and YJ016 (GenBank accession number NP937086) (9). A 13,200-bp ORF homologue of *rtxA* encodes a putative 440-kDa exotoxin designated *rtxA* of *V. anguillarum* (rtx_{Va}). A 462-bp *rtxC*-like gene, designated $rtxC_{Va}$, is upstream of $rtxA_{Va}$ and encodes a putative acylase for $RtxA_{Va}$ activation. Additionally, a 336-bp *rtxH*-like *V. anguillarum* gene, $rtxH_{Va}$, is upstream of $rtxC_{Va}$. Two ORFs located downstream of $rtxA_{Va}$ are homologous to nicotinate-nucleotide-dimethylbenzimidazole phosphoribosyltransferase (ORF1) and cobalamin synthase (ORF2). The sequence of the incomplete ORF was found to be homologous to the *rtxB* gene, an ABC transporter containing an ATP binding cassette that is thought to facilitate the transport of RTX toxins. Sequencing data also revealed that the mini-Tn*10*Km was inserted into this *rtxB* homologue gene (designated $rtxB_{Va}$), which has an orientation opposite to that of $rtxH_{Va}$, $rtxC_{Va}$, and $rtxA_{Va}$ (Fig. 2A).

Since previous studies of other *rtx* operons showed that at least two transport genes exist in *rtx* operons (32), inverse PCR was used to complete the 3′-end sequence of $rtxB_{Va}$ and to identify other possible downstream transporters. Several inverse PCR fragments were obtained (data not shown) and sequenced. The completely sequenced region is available as GenBank accession number EU155486. Analysis of the DNA sequences revealed two additional ORFs downstream of $rtxB_{Va}$ that exhibited strong homology to the ABC transporter proteins (Table 3) and were designated $rtxD_{Va}$ and $rtxE_{Va}$. Both ORFs were located immediately downstream of $rtxB_{Va}$ (Fig. 2). The three putative transport genes ($rtxB_{Va}$, $rtxD_{Va}$, and $rtxE_{Va}$) are transcribed in the same direction and exhibit overlapping regions between the start and stop codons. Like $rtxB_{Va}$, $rtxE_{Va}$ contains an ATP binding cassette region and may act as an ABC transporter. $rtxD_{Va}$ encodes a putative transmembrane fusion protein and is likely part of the ABC transport system for the export of $RtxA_{Va}$ (6, 32). Inverse PCR and DNA sequencing also identified two other ORFs downstream of $rtxE_{Va}$, which are homologous to a chemotaxis gene (ORF3) and a Na-carboxylase symporter gene (ORF4).

***V. anguillarum rtx* operon shares strong homology with other *rtx* operons.** Examination and analysis of the predicted amino acid sequences in the *V. anguillarum rtx* operon by BLASTp (24) revealed important similarities to and differences from other members of the RTX family (Table 3). For example, analysis of the $RtxA_{Va}$ sequence identified a 95% similarity to that of RtxA of *V. vulnificus* and a 90% similarity to that of RtxA of *V. cholerae* El Tor N16961. Besides the *Vibrio* species, sequence analysis of $RtxA_{Va}$ also revealed strong homology with RtxA toxins of other gram-negative bacteria, including the putative cytotoxin RtxA in *Yersinia enterocolitica*, which shares 67% homology with $RtxA_{Va}$. The RtxA toxin in *Aeromonas hydrophila* has a 72% similarity with $RtxA_{Va}$. However, BLASTp analysis did not show significant similarity to HlyA, the RTX toxin/hemolysin of *E. coli* O157:H7 (35). It should be noted that HlyA contains only 998 amino acids (22% as long), compared to the 4,400 amino acids of $RtxA_{Va}$.

In contrast to the RtxA toxins, the activator ($RtxC_{Va}$), the $RtxH_{Va}$, and the secretion ($RtxB_{Va}$, $RtxD_{Va}$, and $RtxE_{Va}$) gene products for $RtxA_{Va}$ share significant similarities among bacterial species. For example, $RtxB_{Va}$ has a homology of 63% to RtxB of *E. coli* O157:H7 and 86% to RtxB of *V. vulnificus* CMCP6. High similarities of transporter proteins indicate that RtxA toxin-related TISSs have been highly conserved in gram-negative bacteria. Interestingly, there are usually three transport genes, *rtxB*, *rtxD*, and *rtxE*, for the secretion of RtxA toxins larger than 350 kDa or 3,200 amino acids in length, like those in *Vibrio*, *Yersinia*, or *Aeromonas* species (Table 3), while only two transport genes, *rtxB* and *rtxD*, are described for the secretion of relatively smaller RtxA toxins, such as those in *B. pertussis*, *E. coli*, and *Pseudomonas* species, which have RtxA toxins with molecular masses of 177 kDa (26), 110 kDa (35), and 55 kDa (3), respectively. Additionally, RtxE proteins are also ATP binding proteins, which share high homology with RtxB. For example, $RtxE_{Va}$ was found to have 64% similarity with RtxB of *E. coli* O157:H7 (Table 3), as well as 84% similarity with RtxE of *V. vulnificus* and *V. cholerae*.

While the arrangement of *rtx* genes in *V. anguillarum* M93Sm was also found to be similar to that of other species, the flanking sequences are quite different, even for other species of *Vibrio* (Fig. 2). Specifically, immediately adjacent to the

TABLE 3—*Continued*

Homology to *rtx* genes of other species[a]							
V. cholerae El Tor N16961				*Yersinia enterocolitica*			
% of identity/ % of similarity	Homologue locus	Putative function	Predicted size (aa)	% of identity/ % of similarity	Homologue locus	Putative function	Predicted size (aa)
85/92	NP_231094	Cytotoxin	4,558	48/67	CAJ90394	Cytotoxin RtxA	3,212
73/88	NP_231093	Rtx acylase	153	51/73	CAJ90393	RtxA activator	152
68/76	NP_231092	Hypothetical protein	119	59/74	CAJ90392	Hypothetical protein	124
66/81	NP_231091	ABC transporter	720	48/65	YP_001006250	ABC transporter	708
63/78	NP_231090	ABC transporter	467	39/60	YP_001006251	ABC transporter	464
72/84	NP_231089	ABC transporter	721	52/70	YP_001006252	ABC transporter	710

rtxE gene of *V. anguillarum* M93Sm there is a putative chemotaxis gene (ORF3). In *V. cholerae*, a histidine kinase/response regulator (VC1445) is adjacent to *rtxE*, while a ubiquitous dehydrogenase (VVA1037) is found in *V. vulnificus* YJ016 (9). On the other side of the *rtx* gene cluster (downstream of *rtxA*), CTX structural genes and bacteriophage elements are present in the *V. cholerae* genome (32), and the *V. vulnificus* YJ016 *rtx* genes are located next to an alanine racemase gene (VVA1029), whereas a cobalamin synthase gene (ORF2) is downstream of the *V. anguillarum* M93Sm *rtxA* gene (Fig. 2).

The *rtx* operon confers hemolytic activity in *V. anguillarum* M93Sm. Mutations were constructed in each *rtx* gene by insertional mutagenesis, as described in Materials and Methods. Examination of each mutant for hemolytic activity revealed that a single mutation in any *rtx* gene gave a hemolytic activity similar to that of the wild-type strain M93Sm (Fig. 1). The results indicated that the loss of any *rtx* gene did not eliminate hemolytic activity, a result which was consistent with the previous report suggesting that *V. anguillarum* contains two hemolysin gene clusters, one of which includes the *vah1* hemolysin gene (40). In order to eliminate the hemolytic effect of *vah1*, a mutation in *vah1* was constructed by allelic exchange. The resulting mutant (S171) had a hemolytic activity similar to that of the wild type, as shown previously (40) (data not shown). The insertional mutation in each of the *rtx* genes was constructed in the S171 background. The *vah1 rtxA*$_{Va}$ double mutant (S183) exhibited a negative hemolytic activity (Fig. 1), which indicated that both *vah1* and *rtxA*$_{Va}$ were required for hemolytic activity in *V. anguillarum* M93Sm. Furthermore, strains carrying the double mutations of *vah1* and any other gene in the *rtx* operon, including *vah1 rtxC*$_{Va}$ (S193), *vah1 rtxB*$_{Va}$ (JR7), *vah1 rtxD*$_{Va}$ (S195), and *vah1 rtxE*$_{Va}$ (S208), all failed to exhibit any hemolytic activity (Fig. 1). This result indicated that all genes in the *rtx* operon were necessary for the hemolytic activity in *V. anguillarum* M93Sm.

Transcriptional analysis of the *rtx*$_{Va}$ operon. RT-PCR was used to discover the transcriptional pattern of the *rtx* genes in *V. anguillarum* M93Sm. Primers complementary to the 3′ end of one gene and the 5′ end of the immediately adjacent downstream gene were used to determine whether transcription resulted in polycistronic mRNA (Table 2 and Fig. 3). RT-PCR data showed that a 646-bp PCR product was amplified with primers crossing the intergenic space of *rtxC*$_{Va}$ and *rtxA*$_{Va}$ (Fig. 3, lane 7), which indicated that *rtxA*$_{Va}$ and *rtxC*$_{Va}$ were transcribed together as a polycistronic mRNA, even with 22 bases between the two genes. Additionally, quantitative RT-PCR showed that *rtxC*$_{Va}$ and *rtxA*$_{Va}$ had similar numbers of transcripts, ~10^6 copies per 100 ng total RNA (data not shown). Furthermore, RT-PCR products of the predicted size were generated between *rtxB*$_{Va}$ and *rtxD*$_{Va}$ (577 bp) and between *rtxD*$_{Va}$ and *rtxE*$_{Va}$ (670 bp) (Fig. 3, lanes 17 and 27, respectively), indicating that the three transporter genes were also transcribed as a polycistronic mRNA, as suggested by sequence analysis, since the three transporter genes overlap each other (Fig. 2A).

Complementation of the *rtx*$_{Va}$ gene mutants. Plasmid constructions were made to complement the *rtx* gene mutants as described previously (40) and shown in Fig. 4A. With the exception of the plasmid constructed for *rtxE*, complementation plasmids for each expression unit were made in two ways: (i) those containing the structural genes plus enough of the upstream sequence to contain the putative native promoter, P$_{native}$; and (ii) those in which the structural genes were inserted behind a strong constitutive promoter for *flaB*, P$_{flaB}$ (7, 17), to drive the genes in question. For *rtxE*, only the putative P$_{native}$ was used. Surprisingly, the plasmid containing the *rtxCH/B* intergenic region plus the *rtxBDE* gene fragment (P$_{native}$-*rtxBDE*) (Fig. 4A) did not restore the hemolytic activities of JR7 (the *vah1 rtxB* double mutant) and S195 (the *vah1 rtxD* double mutant); instead, the plasmid containing the *rtxBDE* genes driven by the constitutive P$_{flaB}$ (P$_{flaB}$-*rtxBDE*) restored the hemolytic activities of both strains JR7 and S195 (Fig. 4). The results suggested the possibility of a regulatory site adjacent to or in the putative native promoter of the *rtxB* gene that is necessary for transcription but does not function in *trans*. Additionally, plasmids harboring the *rtxBD* fragment driven by the *flaB* promoter failed to restore hemolytic activity in either the *vah1 rtxB* (JR7) or the *vah1 rtxD* (S195) double mutant (Fig. 4). This suggested that mutations in *rtxB* or *rtxD* had a polar effect on *rtxE* expression. Similarly, the plasmid harboring the *rtxDE* gene plus its 500-bp upstream region (P$_{native}$-*rtxDE*) (Fig. 4) could not complement the hemolytic activity of *vah1*/*rtxD* mutant (S195), while the *rtxDE* gene, driven by the constitutive P$_{flaB}$ (P$_{flaB}$-*rtxDE*), restored the hemolytic activity of strain S195 (Fig. 4). Surprisingly, the *vah1 rtxE* mutant (S208) complemented with pSUP202 containing *rtxE* plus its 500-bp upstream fragment (P$_{native}$-*rtxE*) completely restored hemolytic activity. This

TABLE 3—*Continued*

Homology to *rtx* genes of other species[a]							
Aeromonas hydrophila subsp. ATCC 7966				*E. coli* O157:H7			
% of identity/ % of similarity	Homologue locus	Putative function	Predicted size (aa)	% of identity/ % of similarity	Homologue locus	Putative function	Predicted size (aa)
57/72	YP_855898	RtxA toxin	4,685	N/A[a]	NP_052622	Hemolysin	998
64/84	YP_855897	Cytolysin-activating lysine-acyltransferase	149	31/56	NP_052623	HlyA acylase	163
69/82	YP_855896	Hypothetical protein	132	N/A[a]			
61/77	YP_855895	ABC transporter	695	47/63	NP_052625	ABC transporter	706
58/76	YP_855894	ABC transporter	454	30/41	NP_052626	ABC transporter	479
67/80	YP_855893	ABC transporter	719	48/64	NP_052625	ABC transporter	706

result indicated that the *rtxE* gene was able to be transcribed from its own native promoter, even though *rtxE* is also transcribed as a polycistronic mRNA together with *rtxB* and *rtxD* (Fig. 3, lane 27).

Plasmids containing the *rtxB*/*HC* intergenic region plus the *rtxC* gene (P_{native}-*rtxC*) or the P_{flaB}-driven *rtxC* gene (P_{flaB}-*rtxC*) (Fig. 4) did not restore the hemolytic activity of strain S193 (the *vah1 rtxC* mutant). Thus, the mutation in *rtxC* had a polar effect on the *rtxA* gene. Attempts to complement the *vah1 rtxA* double mutant were not successful due to the difficulty of cloning and conjugating the 13-kbp-long *rtxA* or *rtxHCA* gene fragment.

Cytotoxic activities of Vah1 and $RtxA_{Va}$ against ASK cells. The RTX toxins produced in *V. cholerae* and other gram-negative bacteria typically display cytotoxic or hemolytic activities (31, 32, 35). In *V. cholerae*, RTX toxin causes HEp-2 cells to round up and detach from surfaces (32). In this study, an ASK cell line was used to test the cytotoxic activity of *V. anguillarum* M93Sm and its various hemolysin mutants. Briefly, ASK cells (~3×10^5 cells/ml) were exposed to *V. anguillarum* cells (MOI, 500) for up to 4 h. As shown in Fig. 5A, more than 99% of the ASK cells were detached and killed ($P < 0.01$) when exposed to washed M93Sm cells. ASK cells also exhibited extensive rounding prior to detachment (Fig. 5B-1). Exposing the ASK cells to washed S171 (the *vah1* deletion mutant) cells also resulted in rounding and a significant decrease in attachment (Fig. 5B-2). After 4 h of exposure to S171 cells, only 8% of the ASK cells were still attached to the surface ($P < 0.01$) compared to that attached to NSS-treated cells. The *rtxA* mutant strain (S123) exhibited weaker cytotoxicity against ASK cells, with about 60% of the cells still attached after treatment ($P < 0.1$). No rounding of the ASK cells was observed when they were treated with S123 cells (Fig. 5B-3). When ASK cells were exposed to the hemolysin-negative strain S183 (the *vah1 rtxA* double mutant), no cytotoxic activity was observed (Fig. 5A) during the 4-h exposure, and ASK cells did not exhibit

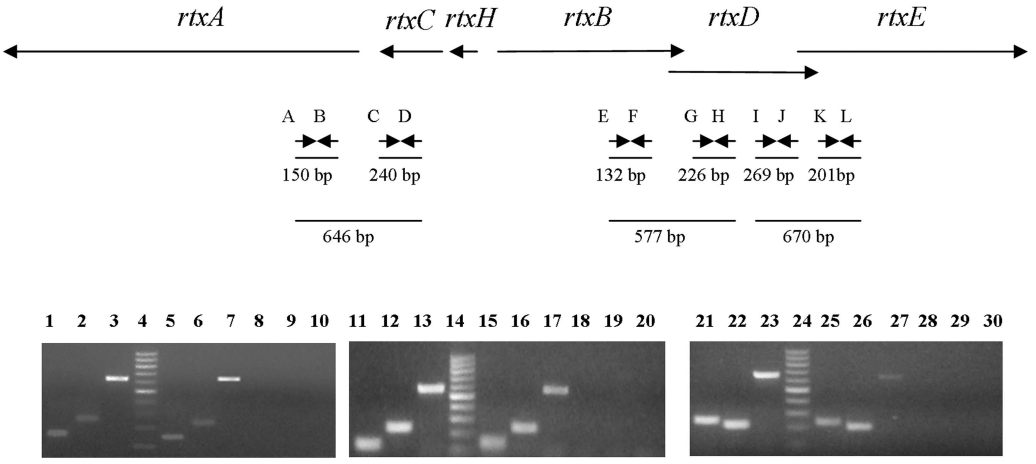

FIG. 3. RT-PCR analysis of transcription from the *rtx* operon in *V. anguillarum* M93Sm. RT-PCR was performed with 100 ng RNA obtained from M93Sm cells grown for 12 h in LB20, using primers labeled as A (Pm112), B (Pm111), C (Pm181), D (Pm180), E (Pm185), F (Pm184), G (Pm183), H (Pm182), I (Pm189), J (Pm187), K (Pm191), and L (Pm190). Lanes 4, 14, and 24, 100-bp molecular marker; lanes 1 to 3, 11 to 13, and 21 to 23, PCRs performed with M93Sm genomic DNA as template served as positive controls; lanes 5 to 7, 15 to 17, and 25 to 27, RT-PCRs performed with 100 ng RNA from 12-h M93Sm cultures. Lanes 8 to 10, 18 to 20, and 28 to 30, PCRs performed without reverse transcriptase, as negative controls. The primers used were as follows: A and B, shown in lanes 1, 5, and 8; C and D, shown in lanes 2, 6, and 9; A and D, shown in lanes 3, 7, and 10; E and F, shown in lanes 11, 15, and 18; G and H, shown in lanes 12, 16, and 19; E and H, shown in lanes 13, 17, and 20; I and J, shown in lanes 21, 25, and 28; K and L, shown in lanes 22, 26, and 29; I and L, shown in lanes 23, 27, and 30. The map of the *rtx* operon shows the locations of the primers used and the lengths of the amplicons obtained.

A)

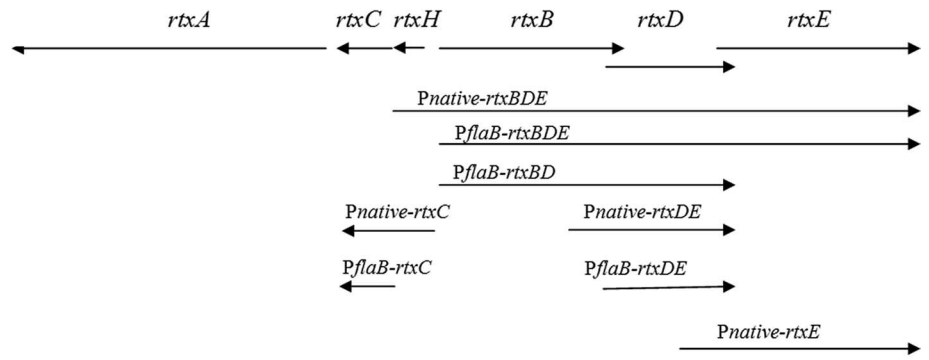

B)

Strain	Transformed plasmid	Hemolytic Activity
M93Sm	None	+
S193 (*vah1 rtxC* mutant)	pSUP202/P_{native}-*rtxC*	-
S193 (*vah1 rtxC* mutant)	pSUP202/P_{flaB}-*rtxC*	-
JR7 (*vah1 rtxB* mutant)	pSUP202/P_{native}-*rtxBDE*	-
JR7 (*vah1 rtxB* mutant)	pSUP202/P_{flaB}-*rtxBDE*	+
JR7 (*vah1 rtxB* mutant)	pSUP202/P_{flaB}-*rtxBD*	-
S195 (*vah1 rtxD* mutant)	pSUP202/P_{flaB}-*rtxBDE*	+
S195 (*vah1 rtxD* mutant)	pSUP202/P_{native}-*rtxDE*	-
S195 (*vah1 rtxD* mutant)	pSUP202/P_{flaB}-*rtxDE*	+
S195 (*vah1 rtxD* mutant)	pSUP202/P_{flaB}-*rtxBD*	-
S208 (*vah1 rtxE* mutant)	pSUP202/P_{native}-*rtxE*	+

FIG. 4. Complementation of the *rtx* mutants and their hemolytic activities. Various gene(s) fragments driven by either a native promoter (P_{native}) or a constitutive promoter (P_{flaB}) (A) were cloned into shuttle vector pSUP202 and introduced into various *V. anguillarum* mutant strains by bacterial mating, as described previously (40). The resulting transconjugants were used to test the hemolytic activities on sheep blood agar plates incubated at 27°C for 48 h, and the relative hemolytic activities were compared with those of the wild-type strain M93Sm (B).

rounding, detachment, or cell death (Fig. 5B-4). The data strongly suggest that while both Vah1 and $RtxA_{Va}$ contribute to the cytotoxicity of *V. anguillarum* cells, ASK cell rounding was observed only when $RtxA_{Va}$ was present. Additionally, the occurrence of ASK cell rounding was observed in the presence of the wild-type M93Sm after only 1 h at a lower MOI value (MOI, 100). It should be noted that at this time and MOI, most ASK cells were still attached and cell viability was similar to that of the NSS-treated cells (data not shown). This suggested that cell rounding precedes cell detachment and death.

Culture supernatants from *V. anguillarum* strains grown overnight in LB20 were collected by centrifugation, passed through a 0.2-μm filter, and tested for cytotoxic activity against ASK cells. ASK cells became highly vacuolated after 4 h of incubation with the M93Sm supernatant; subsequently, ASK cells became rounded and detached when the incubation was continued overnight (Fig. 6, panels M93Sm 4h and M93Sm o/n). This suggested that cell vacuolation and cell rounding are separate events for ASK cells when they are exposed to the *V. anguillarum* supernatant. When the supernatant from S171 (the *vah1* mutant) was added to the ASK cell culture, no vacuolation was observed at any time during the 24-h incubation; however, ASK cells were observed to round up after an overnight (24-h) incubation (Fig. 6, panels *vah1* mutant 4h and *vah1* mutant o/n). This observation suggested that the Vah1 hemolysin was responsible for the vacuolation of ASK cells and that $RtxA_{Va}$ is secreted and is responsible for ASK cell rounding. To confirm these observations, culture supernatants from S123 (the *rtxA* mutant) were added to ASK cells and incubated for 24 h. Vacuolation, but not rounding, of ASK cells was observed in the presence of the S123 supernatant. Furthermore, more vacuoles formed as the incubation time increased (Fig. 6, panels *rtxA* mutant 4h and *rtxA* o/n), which indicated that the Vah1 hemolysin is also a secretory protein and responsible for the vacuolation of ASK cells. When the culture supernatant from S183 (the *vah1 rtxA* double mutant) was added to ASK cells, neither vacuolation nor cell rounding was observed during the 24-h incubation (Fig. 6, panels *vah1 rtxA* double mutant 4h and *vah1 rtxA* double mutant o/n). The same result was obtained when uninoculated LB20 cells (negative control) were added to ASK cells (Fig. 6, panels LB20 4h and LB20 o/n). Taken together, these observations strongly suggest that *vah1* and *rtxA* encode secreted cytotoxins that have different effects upon target cells.

$RtxA_{Va}$ is a major virulence factor to Atlantic salmon. Juvenile Atlantic salmon were infected by i.p. injection with *V. anguillarum* M93Sm and its hemolysin mutants (Table 4) and observed for 21 days. Fish inoculated with $\sim 3 \times 10^6$ CFU of

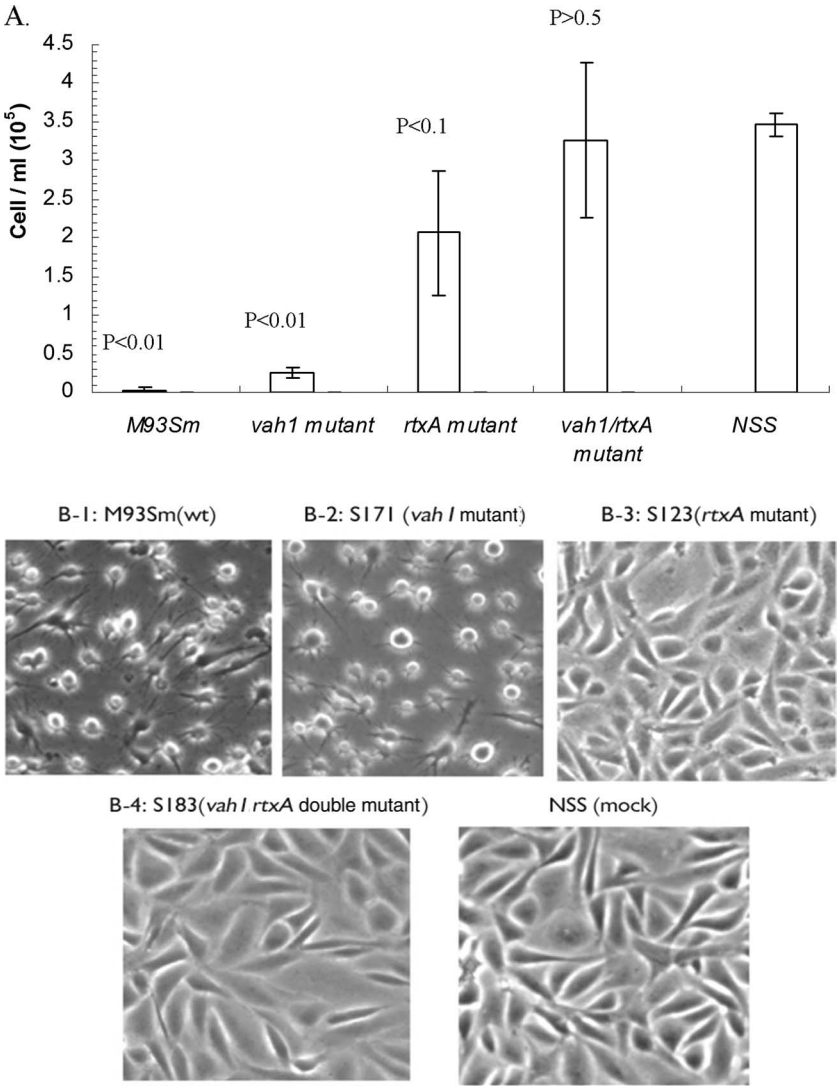

FIG. 5. The cytotoxicity of *V. anguillarum* M93Sm and hemolysin mutant strains against ASK cells. (A) ASK cells were treated with M93Sm and its derivative hemolysin mutants at an MOI of 500 for 4 h. Determination of the ASK cell density and viability is described in Materials and Methods and was carried out using a trypan blue dye exclusion assay. Bars represent the standard deviations of three independent measurements. *P* values above each bar of assays were calculated by *t* test analysis. (B) The morphological changes of treated ASK cells were observed by inverted microscopy at a magnification of ×100. ASK cells were incubated for 1 h with NSS-washed *V. anguillarum* cells at an MOI of 100. The *V. anguillarum* strains added were M93Sm (B-1), S171 (*vah1* mutant) (B-2), S123 (*rtxA* mutant) (B-3), S183 (*vah1 rtxA* double mutant) (B-4), and mock (NSS).

the wild-type strain M93Sm suffered 100% mortality by 3 days, while fish inoculated with ~3×10^5 CFU suffered 60% mortality by 5 days and 40% mortality by 9 days with an inoculation of ~3×10^4 CFU. Similar levels of killing were observed with fish infected with S171 (the *vah1* mutant), with 100% mortality at a dose of 2.9×10^6 CFU, 60% mortality at 2.9×10^5 CFU, and 20% mortality when inoculated with 2.9×10^4 CFU. The data indicated that the *vah1* mutant showed no significant change in virulence compared with the wild-type strain M93Sm. In contrast, no deaths by vibriosis were observed when fish were inoculated with either the *rtxA* mutant S123 or the *vah1 rtxA* double mutant S183. Taken together, these observations strongly suggest that the RtxA hemolysin is a major virulence factor of *V. anguillarum* and that the mutation in *rtxA* results in avirulence to Atlantic salmon.

DISCUSSION

The hemolytic activity of *V. anguillarum* cells has been suggested to be a virulence factor during the infection of fish. The *vah1* gene was the first hemolysin gene identified in *V. anguillarum* (27). Studies demonstrated that *vah1* is distributed widely in *V. anguillarum* strains and is found in serotypes A to I (27); however, additional genes, besides *vah1*, have been found to contribute to the hemolytic activity of *V. anguillarum* cells. Rodkhum et al. (41) demonstrated that there are four additional hemolysin genes (*vah2* to *vah5*) in *V. anguillarum* strain H775-3. Rock and Nelson (40) showed that the mutation of *vah1* had no effect on the hemolytic activity of *V. anguillarum* M93Sm on sheep blood agar, implying that there was an additional hemolysin that contributed to the hemolytic activity

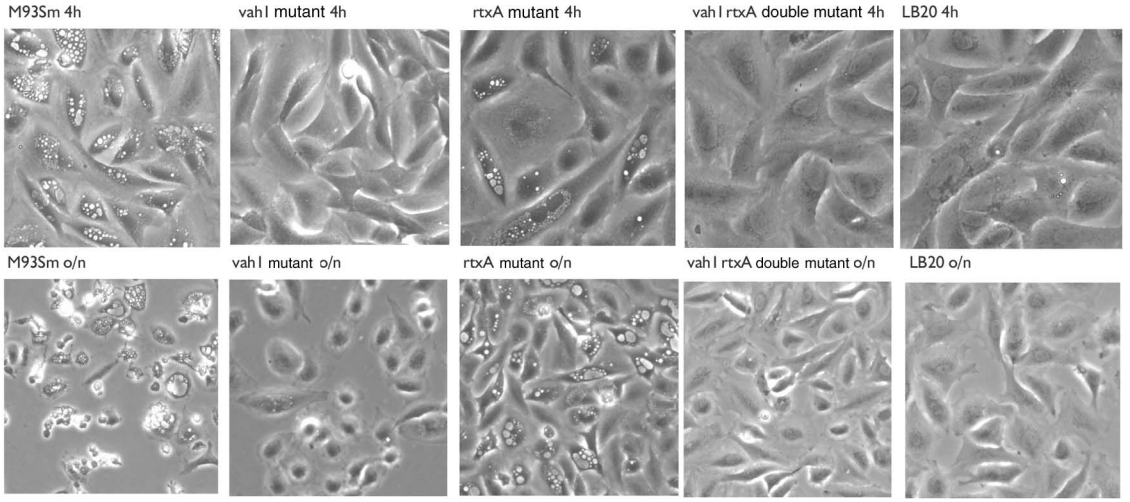

FIG. 6. Morphological changes to ASK cells caused by culture supernatants from the *V. anguillarum* wild-type M93Sm and hemolysin mutant strains observed by inverted microscopy (magnification, ×100). ASK cells were exposed to overnight (o/n) culture supernatants for 4 h (top row) and for 24 h (bottom row). The *V. anguillarum* strains from which the supernatants were obtained are indicated at the top of each photo.

of this strain. Additionally, mutations that knocked out the activity of the adjacent divergently transcribed gene (*plp*) increased hemolytic activity by increasing the transcription of *vah1*. In this study, mini-Tn*10*Km mutagenesis was performed with *V. anguillarum* JR1, a *vah1* knock-out mutant (40) to obtain the hemolysin-negative mutant JR7 (Fig. 1). The regions surrounding the mini-Tn*10*Km insertion were cloned and sequenced, revealing an *rtx* operon with six genes, *rtxACHBDE* (Fig. 2), where *rtxA* encodes the toxin, *rtxC* encodes the toxin activator (acylase), *rtxH* encodes a conserved hypothetical protein, and *rtxBDE* encode three secretion proteins.

Single-insertion mutations created in *rtx* genes did not eliminate hemolytic activity. These single mutants exhibited hemolytic activity similar to that of the wild-type strain M93Sm (Fig. 1). However, double mutations in *vah1* and any of the *rtx* genes resulted in a hemolysis-negative phenotype (Fig. 1), demonstrating that the *rtx* operon is a second hemolysin gene cluster in *V. anguillarum* M93Sm. These data, consistent with that of Rock and Nelson (40), demonstrate that hemolytic activity in *V. anguillarum* M93Sm is the result of two clusters of hemolysin genes, the *vah1* cluster and the *rtx* cluster.

TABLE 4. Virulence of *V. anguillarum* strains in juvenile Atlantic salmon

Strain	Dose/fish (CFU)	Total % of mortality	No. of days until death (no. of fish/total fish)[a]
M93Sm	3.01×10^6	100	2 (2/5), 3 (5/5)
	3.01×10^5	60	3 (2/5), 5 (3/5)
	3.01×10^4	40	6 (1/5), 9 (2/5)
S171 (*vah1* mutant)	2.9×10^6	100	2 (3/5), 3 (5/5)
	2.9×10^5	60	4 (1/5), 5 (3/5)
	2.9×10^4	20	2 (1/5)
S123 (*rtxA* mutant)	1.0×10^6	0	NA[b]
	1.0×10^5	0	NA[b]
	1.0×10^4	0	NA[b]
S183 (*vah1 rtxA* double mutant)	4.7×10^6	0	NA[c]
	4.7×10^5	0	NA[c]
	4.7×10^4	0	NA[b]
Control (NSS)		0	NA[b]

[a] NA, not applicable.
[b] No fish deaths occurred during the 21-day experiment.
[c] One fish in the 4.7×10^6 cells/dose group died at day 8, and two fish in the 4.7×10^5 cells/dose group died at day 12; however, no *V. anguillarum* cells could be isolated on LB20-Sm^{200} plates from the dead fish, and no clinical symptoms of vibriosis were observed.

RTX toxins are a diverse group of protein toxins synthesized by many gram-negative bacteria. Members of the RTX toxin family have been identified as cytolytic toxins, metalloproteases, lipases, and adenylate cyclases. They include *E. coli* hemolysin HlyA (35), *V. cholerae* cytotoxin RtxA (32), *V. vulnificus* cytotoxin RtxA (31), and *B. pertussis* adenylate cyclase CyaA (4, 26). Most RTX toxins are proteins with a molecular mass ranging from 100 kDa to >400 kDa and are posttranslationally activated by acylation via a specific acyltransferase. The repeated structure of RTX toxin proteins, which gave them their name, is composed typically of repeated glycine-rich nonapeptides binding Ca^{2+} on the C-terminal half of the protein (20). The N-terminal sequence of RTX toxins is thought to contain sequences that are responsible for binding to target cells and promoting the formation of cation-selective pores (4, 35). It is interesting that while $RtxA_{Va}$ has typical glycine-rich nonapeptide repeats, closer inspection revealed that the repeats may actually be 18-mer repeats. That is, instead of the usual 9-residue (GGXGXDXXX) repeats, an extra 9 amino acid residues are added to each repeat, resulting in an 18-residue consensus motif, GGXGXDXXVXXGXXNXXX. For $RtxA_{Va}$, these repeats are found at the C-terminal end of the protein (amino acid residues 4031 to 4165) (Fig. 7B). Lin et al. (32) also found 18-residue GD-rich repeats at the C-terminal end of the RtxA toxin of *V. cholerae*. Additionally, we found that $RtxA_{Va}$ contains a novel 19-amino-acid repeat with the consensus motif GX(A/G)N(I/V)XT(K/H)VGDGXXXXXXX ($RtxA_{Va}$, amino acids 784 to 1354) (Fig. 7A). This novel 19-amino-acid repeat is very similar to the 19-amino-acid repeat found in *V. cholerae*, with the consensus sequence of GXAN(I/V)XT(K/H)V GDGXTVAVMX (32). Recently, Satchell (42) demonstrated

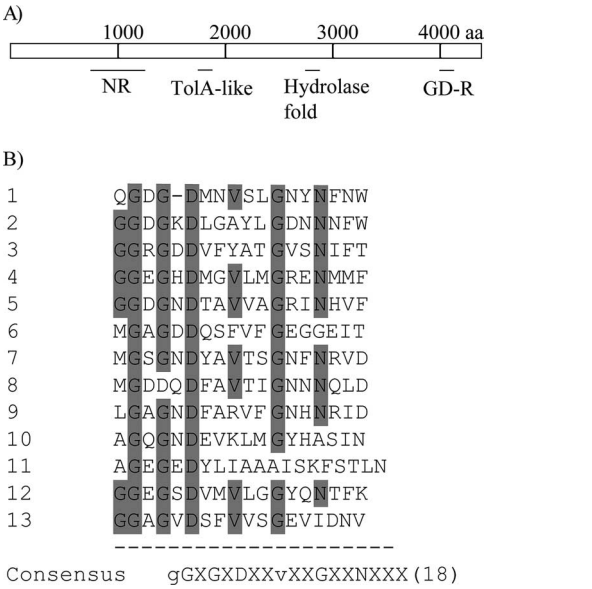

FIG. 7. Features of $RtxA_{Va}$ toxin. (A) Conserved domains found in $RtxA_{Va}$. NR, novel repeat or B-repeat (amino acids 784 to 1354); Tol-A like, domain (amino acids 1609 to 1868); Hydrolase fold, amino acids 2728 to 2808; GD-R, GD-rich repeat or C repeat (amino acids 4031 to 4265). (B) The GD-rich repeats and consensus sequences found in the C-terminal portion of $RtxA_{Va}$. Gray highlights indicate the consensus repeat residues.

that MARTX toxins are distinguished from other RTX toxins by the large number of primary sequences composed of glycine-rich repeats. The author noted that there are three conserved repeat regions in the MARTX toxin family, termed the A, B, and C repeats. The A repeats are 20-amino-acid repeats located near the N terminus. The B repeats (originally novel repeats) are 19-amino-acid repeats just downstream of the A repeats. The C repeats are 18-amino-acid GD-rich repeats of the C-terminal region. Similar repeat regions in the *rtxA* gene indicate that $RtxA_{Va}$ also is a member of MARTX toxin family. We also found two conserved domains by using a search of the CDD (34). One domain is located at amino acid residues 2728 to 2808 and appears to be an alpha/beta hydrolase fold (NCBI Conserved Domains database no. pfam00561). The other domain is located at amino acid residues 1609 to 1868. This domain is similar to a TolA-like protein (pfam06519). The function of these domains in $RtxA_{Va}$ toxin is unknown.

In *V. cholerae*, RtxA functions as cytotoxin that causes cell rounding and depolymerization of actin stress fibers in a broad range of cell types. The depolymerized actin monomers are covalently cross-linked into polymers (22, 32). In our studies, *V. anguillarum* strains containing an intact *rtxA* gene (M93Sm or S171) caused ASK cells to round, detach, and die (Fig. 5). No rounding was observed with ASK cells treated with strains lacking a functional *rtxA* gene (S123 or S183). It has been shown for RtxA of *V. cholerae* that an ACD is responsible for actin cross-linking but not for cell rounding (11, 43). Furthermore, analysis of RtxA sequences from both *V. vulnificus* (43) and *V. anguillarum* reveals that neither protein contains an ACD. These analyses are consistent with those of Sheahan and Satchell (44; unpublished data in Cordero et al. [12]), who were unable to detect actin cross-linking by *V. vulnificus* RtxA. Similarly, we were also unable to detect actin cross-linking by *V. anguillarum* RtxA (data not shown). However, as noted above, the RtxA toxin of both *V. vulnificus* (31) and *V. anguillarum* M93Sm (Fig. 5 and 6) causes target cell rounding, which implies that cell rounding caused by the RtxA of *Vibrio* species is triggered by a domain common to all *Vibrio* RtxA toxins. Interestingly, deletion of the ACD domain from the RtxA of *V. cholerae* does not completely eliminate the ability to cause cell rounding in target cells. The resulting slow cell rounding is thought to occur due to the inactivation of small Rho GTPases by the Rho inactivation domain (RID) in RtxA of *V. cholerae* (44). A homologue of the RID domain was also identified in $RtxA_{Va}$; however, the contribution of the RID to cell rounding and cytotoxicity by $RtxA_{Va}$ needs to be investigated further.

The cytotoxicity assay using ASK cells revealed that Vah1 and $RtxA_{Va}$ are both exotoxins and each has a distinct effect on ASK cells. Our data demonstrate that the culture supernatant from an overnight culture of S171 (the *vah1* mutant) caused ASK cell rounding, while the culture supernatant from S123 (the *rtxA* mutant) caused ASK cell vacuolation (Fig. 6). Culture supernatants from M93Sm caused both rounding and vacuolation, while supernatants from S183 (the *rtxA vah1* double mutant) had no effect on ASK cells. Previously, it was found that the HlyA hemolysin of *V. cholerae* causes vacuolation in many types of eukaryotic cells (10, 19, 38). HlyA shares strong homology (76%) with Vah1 of *V. anguillarum*. Chakraborty et al. (8) also indentified a cytotoxin in *V. fluvialis* which has 81% homology to HlyA of *V. cholerae* and also causes the vacuolation of HeLa cells. Taken together, the data strongly suggest that Vah1 of *V. anguillarum* M93Sm causes vacuolation of ASK cells. The data also suggest that the two hemolysins/cytotoxins Vah1 and RtxA have different mechanisms for cytotoxic activity and that the two toxins work synergistically to increase the cytotoxicity of M93Sm for ASK cells (Fig. 5A).

Our fish infection studies (Table 4) revealed that *rtxA* is a major contributor of virulence. Strains of *V. anguillarum* that lacked a functional *rtxA* gene were avirulent. In contrast, the *vah1* mutant strain S171 exhibited no decrease in virulence compared to the wild-type strain M93Sm. These results are similar to those of Fullner et al. (21) for *V. cholerae* in which RtxA was found to be a major accessory toxin. However, the deletion of *hlyA* (a homologue of *vah1*) from *V. cholerae* did not affect virulence in the murine pulmonary model, but *hlyA* contributed predominately to the virulence in the adult mouse intestinal infection model, with *rtxA* playing a secondary role (39). In contrast, the Vvh toxin of *V. vulnificus*, also a homologue of Vah1, is thought to contribute directly to virulence by causing vasodilation and hypotensive septic shock (30). Our data clearly show that $RtxA_{Va}$ is a major virulence factor in fish infection by i.p. injection. Additionally, $RtxA_{Va}$ appears to have a strong cytotoxic effect against fish erythrocyte and macrophage cells (unpublished data). It will be interesting to discover whether RtxA plays a role during the initial invasion of the fish across the intestinal epithelium during infections of fish by immersion or anal intubation.

It is interesting to note that while *rtx* gene clusters in *Vibrio* species are highly conserved, retaining strong protein homologies and gene arrangements (Fig. 2 and Table 3), the flanking genes surrounding the *rtx* genes differ among *V. cholerae*, *V. vulnificus*, and *V. anguillarum* (Fig. 2). Lin et al. (32) demon-

strated that the *rtx* operon in *V. cholerae* is adjacent to the CTX prophage and is considered part of a pathogenicity island. However, they also found that the 5′ end of *rtxA*, all of *rtxC*, and the 5′ end of *rtxB* were deleted in classical biotypes of *V. cholerae*. The authors suggested that the acquisition of the *rtx* operon predated the acquisition of the CTX element. In contrast, the *rtx* operons in both *V. anguillarum* and *V. vulnificus* are flanked by different sets of housekeeping genes and are not associated with obvious pathogenicity islands. The similarity of *rtx* operons and the distinct flanking sequences among *Vibrio* species suggests that the *rtx* operon was probably transferred horizontally between *Vibrio* species.

Rtx toxins are secreted by a TISS (6), which consists of an ATP-binding protein (i.e., $RtxB_{Va}$ and $RtxE_{Va}$) and a membrane-fusion protein ($RtxD_{Va}$). In *V. anguillarum*, the deduced amino acid sequences of the three secretion proteins (encoded by $rtxBDE_{Va}$) of the *rtx* operon show high degrees of amino acid sequence similarity with other *rtx* operons. For example, for $rtxB_{Va}$ the deduced encoded protein sequence has a 63% similarity to that of *E. coli* HlyB and an 81% similarity to that of *V. vulnificus* RtxB (Table 3). Comparison of the *rtx* secretion genes from various bacterial species revealed an interesting difference among the secretion systems regarding the presence or absence of *rtxE*. We found, using BLASTx, that *rtxE* is broadly distributed among *rtx* operons that contain the larger versions of RtxA (>3,000 amino acid residues long), such as those found in *Vibrio*, *Yersinia*, and *Aeromonas* species (Table 3), while *rtxE* is not found in *rtx* operons with smaller RtxA proteins, such as those in *E. coli*, *B. pertussis*, and *Pasteurella* species. Boardman and Satchell (6) suggested that the secretion system containing *rtxE* is an atypical TISS and thought that RtxB and RtxE might form a heterodimer during the secretion of RtxA in *V. cholerae*. Our data suggest that a similar secretion mechanism exists in *V. anguillarum*. Furthermore, secretion of RtxA also requires an additional unlinked gene, *tolC* (5). However, we have not yet identified a *tolC* homologue in *V. anguillarum* M93Sm.

Finally, our data indicate that *rtxC* and *rtxA* are cotranscribed, as are *rtxB*, *rtxD*, and *rtxE*. We also found an *rtxH* homologue, which Liu et al. (33) demonstrated was cotranscribed with *rtxC* and *rtxA* in *V. vulnificus*. The regulation of *rtx* transcription by *rtxH* or other factors is currently under investigation.

ACKNOWLEDGMENT

This work was supported by the National Research Initiative of the USDA Cooperative State Research, Education, and Extension Service, grant no. 2005-35204-16294, awarded to D.R.N.

REFERENCES

1. **Austin, B., and D. A. Austin.** 1999. Characteristics of the pathogens. Bacterial fish pathogens: disease of farmed and wild fish, 3rd ed. Praxis Publishing Co., London, United Kingdom.
2. **Bauer, M. E., and R. A. Welch.** 1996. Characterization of an RTX toxin from enterohemorrhagic *Escherichia coli* O157:H7. Infect. Immun. **64:**167–175.
3. **Baumann, U., S. Wu, K. M. Flaherty, and D. B. McKay.** 1993. Three-dimensional structure of the alkaline protease of *Pseudomonas aeruginosa*: a two-domain protein with a calcium binding parallel beta roll motif. EMBO J. **12:**3357–3364.
4. **Benz, R., E. Maier, D. Ladant, A. Ullmann, and P. Sebo.** 1994. Adenylate cyclase toxin (CyaA) of Bordetella pertussis. Evidence for the formation of small ion-permeable channels and comparison with HlyA of *Escherichia coli*. J. Biol. Chem. **269:**27231–27239.
5. **Bina, J. E., and J. J. Mekalanos.** 2001. *Vibrio cholerae tolC* is required for bile resistance and colonization. Infect. Immun. **69:**4681–4685.
6. **Boardman, B. K., and K. J. Satchell.** 2004. *Vibrio cholerae* strains with mutations in an atypical type I secretion system accumulate RTX toxin intracellularly. J. Bacteriol. **186:**8137–8143.
7. **Carroll, J. A., P. E. Stewart, P. Rosa, A. F. Elias, and C. F. Garon.** 2003. An enhanced GFP reporter system to monitor gene expression in *Borrelia burgdorferi*. Microbiology **149:**1819–1828.
8. **Chakraborty, R., S. Chakraborty, K. De, S. Sinha, A. K. Mukhopadhyay, J. Khanam, T. Ramamurthy, Y. Takeda, S. K. Bhattacharya, and G. B. Nair.** 2005. Cytotoxic and cell vacuolating activity of *Vibrio fluvialis* isolated from paediatric patients with diarrhoea. J. Med. Microbiol. **54:**707–716.
9. **Chen, C. Y., K. M. Wu, Y. C. Chang, C. H. Chang, H. C. Tsai, T. L. Liao, Y. M. Liu, H. J. Chen, A. B. Shen, J. C. Li, T. L. Su, C. P. Shao, C. T. Lee, L. I. Hor, and S. F. Tsai.** 2003. Comparative genome analysis of *Vibrio vulnificus*, a marine pathogen. Genome Res. **13:**2577–2587.
10. **Coelho, A., J. R. Andrade, A. C. Vicente, and V. J. Dirita.** 2000. Cytotoxic cell vacuolating activity from *Vibrio cholerae* hemolysin. Infect. Immun. **68:**1700–1705.
11. **Cordero, C. L., D. S. Kudryashov, E. Reisler, and K. J. Satchell.** 2006. The actin cross-linking domain of the *Vibrio cholerae* RTX toxin directly catalyzes the covalent cross-linking of actin. J. Biol. Chem. **281:**32366–32374.
12. **Cordero, C. L., S. Sozhamannan, and K. J. Satchell.** 2007. RTX toxin actin cross-linking activity in clinical and environmental isolates of *Vibrio cholerae*. J. Clin. Microbiol. **45:**2289–2292.
13. **Denkin, S. M., and D. R. Nelson.** 1999. Induction of protease activity in *Vibrio anguillarum* by gastrointestinal mucus. Appl. Environ Microbiol. **65:**3555–3560.
14. **Denkin, S. M., and D. R. Nelson.** 2004. Regulation of *Vibrio anguillarum empA* metalloprotease expression and its role in virulence. Appl. Environ. Microbiol. **70:**4193–4204.
15. **Denkin, S. M., P. Sekaric, and D. R. Nelson.** 2004. Gel shift analysis of the *empA* promoter region in *Vibrio anguillarum*. BMC Microbiol. **4:**42.
16. **Di Lorenzo, M., M. Stork, M. E. Tolmasky, L. A. Actis, D. Farrell, T. J. Welch, L. M. Crosa, A. M. Wertheimer, Q. Chen, P. Salinas, L. Waldbeser, and J. H. Crosa.** 2003. Complete sequence of virulence plasmid pJM1 from the marine fish pathogen *Vibrio anguillarum* strain 775. J. Bacteriol. **185:**5822–5830.
17. **Eggers, C. H., M. J. Caimano, M. L. Clawson, W. G. Miller, D. S. Samuels, and J. D. Radolf.** 2002. Identification of loci critical for replication and compatibility of a *Borrelia burgdorferi* cp32 plasmid and use of a cp32-based shuttle vector for the expression of fluorescent reporters in the Lyme disease spirochaete. Mol. Microbiol. **43:**281–295.
18. **Egidius, E.** 1987. Vibriosis: pathogenicity and pathology. Aquaculture **7:**15–28.
19. **Figueroa-Arredondo, P., J. E. Heuser, N. S. Akopyants, J. H. Morisaki, S. Giono-Cerezo, F. Enriquez-Rincon, and D. E. Berg.** 2001. Cell vacuolation caused by *Vibrio cholerae* hemolysin. Infect. Immun. **69:**1613–1624.
20. **Frey, J., and P. Kuhnert.** 2002. RTX toxins in *Pasteurellaceae*. Int. J. Med. Microbiol. **292:**149–158.
21. **Fullner, K. J., J. C. Boucher, M. A. Hanes, G. K. Haines, 3rd, B. M. Meehan, C. Walchle, P. J. Sansonetti, and J. J. Mekalanos.** 2002. The contribution of accessory toxins of *Vibrio cholerae* O1 El Tor to the proinflammatory response in a murine pulmonary cholera model. J. Exp. Med. **195:**1455–1462.
22. **Fullner, K. J., and J. J. Mekalanos.** 2000. In vivo covalent cross-linking of cellular actin by the *Vibrio cholerae* RTX toxin. EMBO J. **19:**5315–5323.
23. **Garcia, T., K. Otto, S. Kjelleberg, and D. R. Nelson.** 1997. Growth of *Vibrio anguillarum* in salmon intestinal mucus. Appl. Environ. Microbiol. **63:**1034–1039.
24. **Gish, W., and D. J. States.** 1993. Identification of protein coding regions by database similarity search. Nat. Genet. **3:**266–272.
25. **Herrero, M., V. de Lorenzo, and K. N. Timmis.** 1990. Transposon vectors containing non-antibiotic resistance selection markers for cloning and stable chromosomal insertion of foreign genes in gram-negative bacteria. J. Bacteriol. **172:**6557–6567.
26. **Hewlett, E. L., K. J. Kim, S. J. Lee, and M. C. Gray.** 2000. Adenylate cyclase toxin from *Bordetella pertussis*: current concepts and problems in the study of toxin functions. Int. J. Med. Microbiol. **290:**333–335.
27. **Hirono, I., T. Masuda, and T. Aoki.** 1996. Cloning and detection of the hemolysin gene of *Vibrio anguillarum*. Microb. Pathog. **21:**173–182.
28. **Jansen, R., J. Briaire, E. M. Kamp, A. L. Gielkens, and M. A. Smits.** 1993. Cloning and characterization of the *Actinobacillus pleuropneumoniae*-RTX-toxin III (ApxIII) gene. Infect. Immun. **61:**947–954.
29. **Jansen, R., J. Briaire, E. M. Kamp, A. L. Gielkens, and M. A. Smits.** 1993. Structural analysis of the *Actinobacillus pleuropneumoniae*-RTX-toxin I (ApxI) operon. Infect. Immun. **61:**3688–3695.
30. **Kook, H., S. E. Lee, Y. H. Baik, S. S. Chung, and J. H. Rhee.** 1996. *Vibrio vulnificus* hemolysin dilates rat thoracic aorta by activating guanylate cyclase. Life Sci. **59:**PL41–PL47.
31. **Lee, J. H., M. W. Kim, B. S. Kim, S. M. Kim, B. C. Lee, T. S. Kim, and S. H. Choi.** 2007. Identification and characterization of the *Vibrio vulnificus rtxA* essential for cytotoxicity in vitro and virulence in mice. J. Microbiol. **45:**146–152.
32. **Lin, W., K. J. Fullner, R. Clayton, J. A. Sexton, M. B. Rogers, K. E. Calia,**

S. B. Calderwood, C. Fraser, and J. J. Mekalanos. 1999. Identification of a *Vibrio cholerae* RTX toxin gene cluster that is tightly linked to the cholera toxin prophage. Proc. Natl. Acad. Sci. USA **96:**1071–1076.
33. **Liu, M., A. F. Alice, H. Naka, and J. H. Crosa.** 2007. The HlyU protein is a positive regulator of *rtxA1*, a gene responsible for cytotoxicity and virulence in the human pathogen *Vibrio vulnificus*. Infect. Immun. **75:**3282–3289.
34. **Marchler-Bauer, A., and S. H. Bryant.** 2004. CD-search: protein domain annotations on the fly. Nucleic Acids Res. **32**(Web server issue)**:**W327–W331.
35. **Menestrina, G., C. Moser, S. Pellet, and R. Welch.** 1994. Pore-formation by *Escherichia coli hemolysin* (HlyA) and other members of the RTX toxins family. Toxicology **87:**249–267.
36. **Milton, D. L., A. Norqvist, and H. Wolf-Watz.** 1992. Cloning of a metalloprotease gene involved in the virulence mechanism of *Vibrio anguillarum*. J. Bacteriol. **174:**7235–7244.
37. **Milton, D. L., R. O'Toole, P. Horstedt, and H. Wolf-Watz.** 1996. Flagellin A is essential for the virulence of *Vibrio anguillarum*. J. Bacteriol. **178:**1310–1319.
38. **Mitra, R., P. Figueroa, A. K. Mukhopadhyay, T. Shimada, Y. Takeda, D. E. Berg, and G. B. Nair.** 2000. Cell vacuolation, a manifestation of the El Tor hemolysin of *Vibrio cholerae*. Infect. Immun. **68:**1928–1933.
39. **Olivier, V., G. K. Haines III, Y. Tan, and K. J. Satchell.** 2007. Hemolysin and the multifunctional autoprocessing RTX toxin are virulence factors during intestinal infection of mice with *Vibrio cholerae* El Tor O1 strains. Infect. Immun. **75:**5035–5042.
40. **Rock, J. L., and D. R. Nelson.** 2006. Identification and characterization of a hemolysin gene cluster in *Vibrio anguillarum*. Infect. Immun. **74:**2777–2786.
41. **Rodkhum, C., I. Hirono, J. H. Crosa, and T. Aoki.** 2005. Four novel hemolysin genes of *Vibrio anguillarum* and their virulence to rainbow trout. Microb. Pathog. **39:**109–119.
42. **Satchell, K. J.** 2007. MARTX, multifunctional autoprocessing repeats-in-toxin toxins. Infect. Immun. **75:**5079–5084.
43. **Sheahan, K. L., C. L. Cordero, and K. J. Satchell.** 2004. Identification of a domain within the multifunctional *Vibrio cholerae* RTX toxin that covalently cross-links actin. Proc. Natl. Acad. Sci. USA **101:**9798–9803.
44. **Sheahan, K. L., and K. J. Satchell.** 2007. Inactivation of small Rho GTPases by the multifunctional RTX toxin from *Vibrio cholerae*. Cell. Microbiol. **9:**1324–1335.
45. **Toranzo, A. E., and J. L. Barja.** 1993. Virulence factors of bacteria pathogenic for coldwater fish. Annu. Rev. Fish Dis. **3:**5–36.

Editor: V. J. DiRita